General Disclaimer

One or more of the Following Statements may affect this Document

- This document has been reproduced from the best copy furnished by the organizational source. It is being released in the interest of making available as much information as possible.

- This document may contain data, which exceeds the sheet parameters. It was furnished in this condition by the organizational source and is the best copy available.

- This document may contain tone-on-tone or color graphs, charts and/or pictures, which have been reproduced in black and white.

- This document is paginated as submitted by the original source.

- Portions of this document are not fully legible due to the historical nature of some of the material. However, it is the best reproduction available from the original submission.

NASA CR-144979

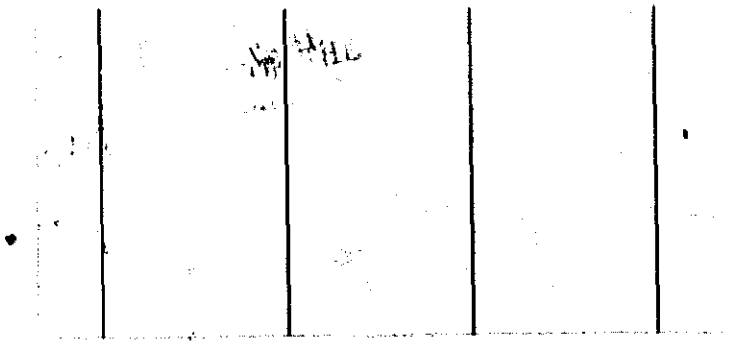

General Applied Science Laboratories inc.

NASA CR-144979

EXPERIMENTAL INVESTIGATION OF WALL SHOCK CANCELLATION AND REDUCTION OF WALL INTERFERENCE IN TRANSONIC TESTING

By Antonio Ferri and Gerald Roffe

Prepared under Contract No. NAS1-13616

GENERAL APPLIED SCIENCE LABORATORIES, INC.
Merrick and Stewart Avenues
Westbury, New York 11590

for

NATIONAL AERONAUTICS AND SPACE ADMINISTRATION

TABLE OF CONTENTS

LIST OF FIGURES

LIST OF FIGURES (Continued)

ABSTRACT

A series of experiments were performed to evaluate the effectiveness of a three-dimensional land and groove wall geometry and a variable permeability distribution to reduce the interference produced by the porous walls of a supercritical transonic test section. The three-dimensional wall geometry was found to diffuse the pressure perturbations caused by small local mismatches in wall porosity permitting the use of a relatively coarse wall porosity control to reduce or eliminate wall interference effects. The wall porosity distribution required was found to be a sensitive function of Mach number requiring that the Mach number repeatability characteristics of the test apparatus be quite good. The effectiveness of a variable porosity wall is greatest in the upstream region of the test section where the pressure differences across the wall are largest. An effective variable porosity wall in the downstream region of the test section requires the use of a slightly convergent test section geometry.

I. INTRODUCTION

In principle, the flow near the wall of a transonic test section can be controlled by altering the local wall properties (permeability and/or shape) to eliminate wall interference (Reference 1). The concept, known as the "intelligent wall", is based on measuring local flow properties near the wall, comparing them with those predicted for an interference-free flow and correcting wall properties until differences between the actual and interference-free flow disappear along the wall boundary. Although the concept applies to both subsonic and transonic flows, its application to the latter is made difficult by the extreme sensitivity which Mach number, and thus wave propagation angle, displays toward flow deflection disturbances.

In principle, any wave reaching a permeable test section wall can be cancelled at the wall by selecting an appropriate local value of wall permeability. However, if the wall permeability is not properly matched to the wave strength the wave will be reflected, either as a compression or an expansion, depending upon the sign of the permeability mismatch. When one considers the cancellation of a simple two-dimensional wave reaching a wall, the problem is rather simple and requires only that the appropriate value of wall permeability be selected. However, when one considers more common situations such as the intersection of the bow wave of an axially symmetric model with a wall, the problem becomes more complex. In this case, the bow wave system consists of a shock followed by an isentropic compression of nearly equal strength. If the wall permeability were to be selected so as to cancel the reflection of the shock, the family of following compression waves would be reflected as expansions, disturbing the model flow field. If the wall permeability were to be selected so as to cancel the isentropic compression fan, the leading shock would reflect, again causing a disturbance.

In general, there are two approaches to solving this problem: tailoring the wall permeability distribution so as to exactly match the requirements imposed by the intersecting flow field or selecting a uniform value of permeability appropriate to the total strength of the distributed shock-

compression system. The mechanics of implementing the first approach are made extremely complex by the fact that the bow wave system is a surface which intersects the wall along a curved line and small changes in test section Mach number produce significant movement of the wall-wave intersection curve. The second approach is far simpler mechanically and must eventually produce cancellation at large distances from the intersection zone. However, close to the intersection region, the mismatch produces a weakened shock followed by an expansion fan of the same family which propagate into the flow field and can cause significant disturbances.

In the work reported here, an alternate concept has been explored for controlling the reflection of nonuniform wave systems from the permeable walls of a transonic test section. Fundamental to this concept is the use of a uniform wall permeability in the region of the bow wave system intersection in order to avoid mechanical complexity. However, the flow field disturbances normally associated with the local mismatch of wall permeability are rapidly cancelled by the use of a three-dimensional wall geometry which diffuses the wave system in the streamwise direction. The technique permits introducing wall permeability corrections in a rather simple way without the need to produce extremely close matching of streamwise gradients, as long as the average local permeability is correct. Moreover, the method is applicable to adjusting flow field properties throughout the test section and can be employed to allow implementation of the intelligent wall concept in a mechanically realistic way.

The details of this interference control scheme will be discussed in the next section. A series of experiments have been conducted to determine its effectiveness at supersonic free stream Mach numbers close to one. This report describes these experiments, presents their detailed results and draws conclusions regarding the applicability of the technique of three-dimensional wall geometry and tailored wall porosity for minimizing wall interference effects in transonic testing.

II. INTERFERENCE CONTROL TECHNIQUE

The fundamental mechanism used to control test section wall interference is that of variable wall permeability. If a compression wave were to strike a solid surface, the condition of flow tangency requires that it reflect as a compression. If, on the other hand, the compression wave were to strike a free boundary, the condition of constant boundary pressure requires that it reflect as an expansion. Clearly, by varying the wall permeability between zero (solid wall) and one (open test section) one can always find a value for which the wave reflection changes from compression to expansion at which point the wave reflects as a Mach wave of zero strength.

For an ideal wall, the particular value of wall permeability required for the zero reflection condition is not a function of the strength of the wave. However, real walls display cross flow characteristics which vary with wave strength and type. As a result, achieving a zero reflection condition in a real test section requires tailoring the wall permeability to the intersecting flow field. Since close tailoring is extremely difficult, a mechanism must be employed to decrease the sensitivity to local permeability mismatches, as long as the average permeability within a given region is correct. The mechanism employed here consists of diffusing a concentrated wave system in the streamwise direction by the use of a simple three-dimensional wall geometry. To understand the functioning of this system, consider the solid corrugated test section wall illustrated in Figure (1). For convenience, the inner and outer wall surfaces will be referred to as lands and grooves, respectively.

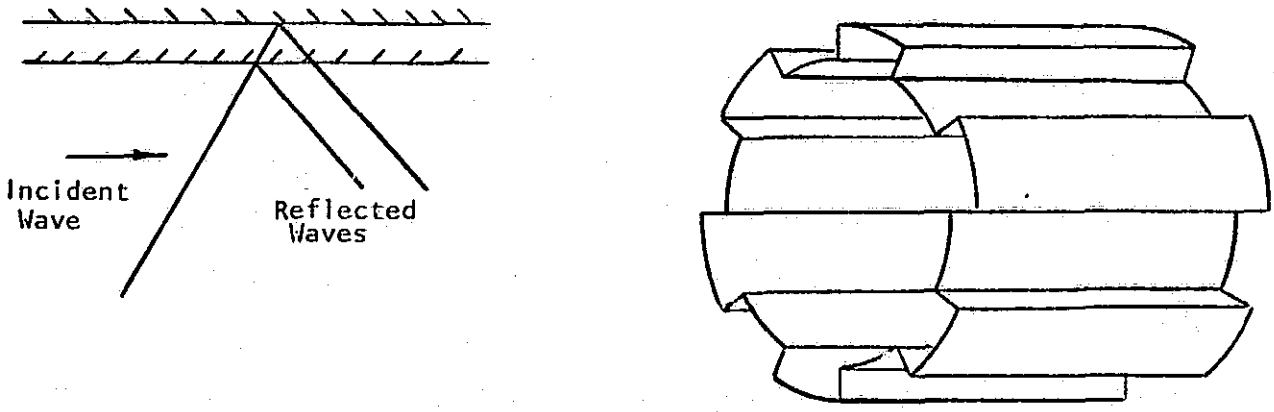

FIGURE 1. WAVE REFLECTION FROM A CORRUGATED SURFACE

A two-dimensional shock reaching the wall reflects from the inner or land surface producing the expected two-dimensional pressure rise immediately downstream of the intersection point. However, this results in a lateral pressure gradient which turns the air toward the grooves, weakening the reflected shock. Reflection of the shock from the groove surface occurs further downstream and is strengthened by the flow spillage from the land surface to produce the final expected two-dimensional pressure rise. The net result is a geometric spreading of the two-dimensional pressure rise over a streamwise distance proportional to the depth of the grooves and a corresponding decrease in the streamwise pressure gradient.

Since the pressure rise produced across a bow wave system is small at transonic speeds, the use of a corrugated wall design can distribute the pressure rise over a distance sufficient to produce gradients which are of the same order as those encountered elsewhere in the flow. As a result, gradually distributed variable porosity can be used to produce the correct wall conditions. At the same time an average porosity value can be selected using the same criteria used for the gradual pressure variations encountered elsewhere in the flow.

The use of a three-dimensional wall geometry provides the possibility of using wall corrections to eliminate wall interference in the presence of shocks. Figure (2) illustrates a possible scheme for such an approach using a corrugated wall made up of a series of parallel channels of unequal depth. The flow field created by such a wall is illustrated schematically in Figure (3).

The incident wave w_1 strikes surfaces A, B and C at positions which are displaced in the streamwise direction by an amount proportional to the difference in their radial positions. The wave is of a strength which causes a flow deflection δ. The pressure perturbation immediately behind the reflection of the wave on surface A is proportional to 2δ. However, the pressure at radial station B adjoining this surface is still δ, causing expansion waves to propagate laterally inward lowering the pressure on A, turning the flow outward to spill over onto surface B and weakening reflected wave w_2. The pressure increase on surface B is somewhat larger than that on A due to the increased pressure caused by the initial spillover. However, the initial

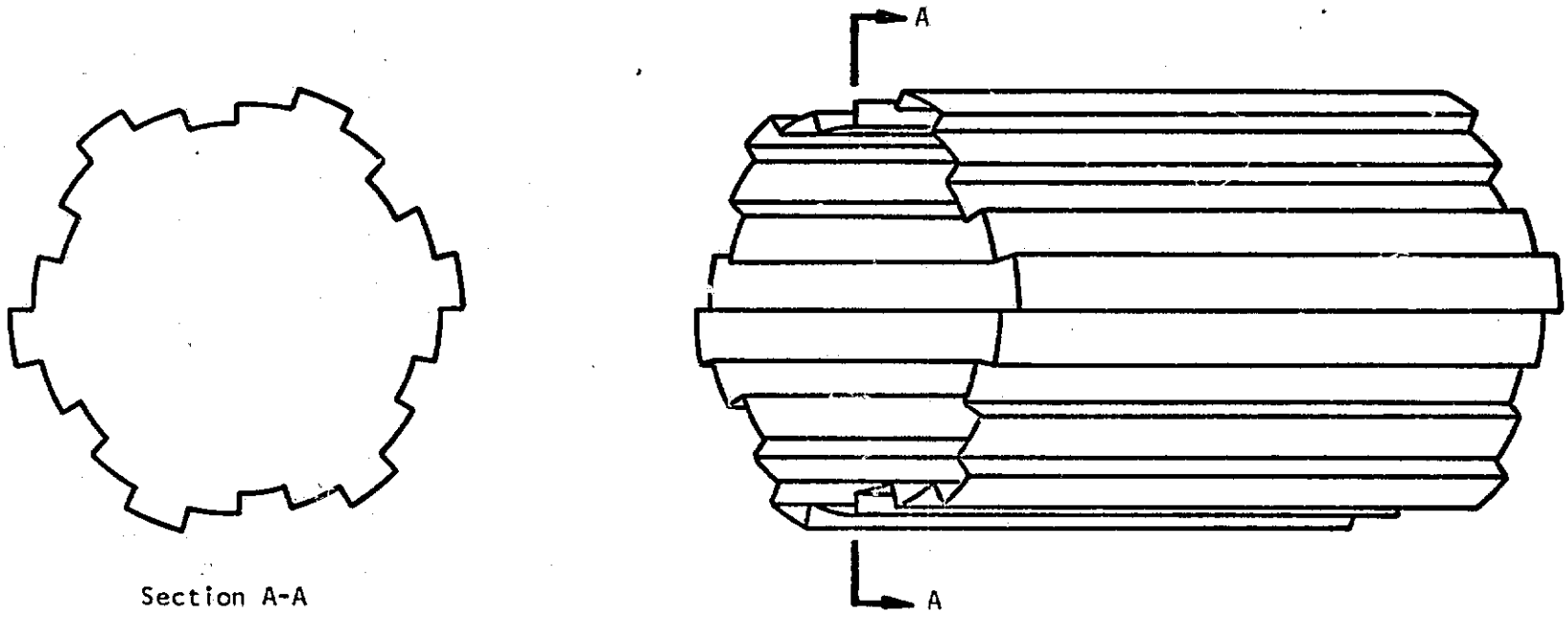

FIGURE 2. MULTICHANNEL CORRUGATED WALL

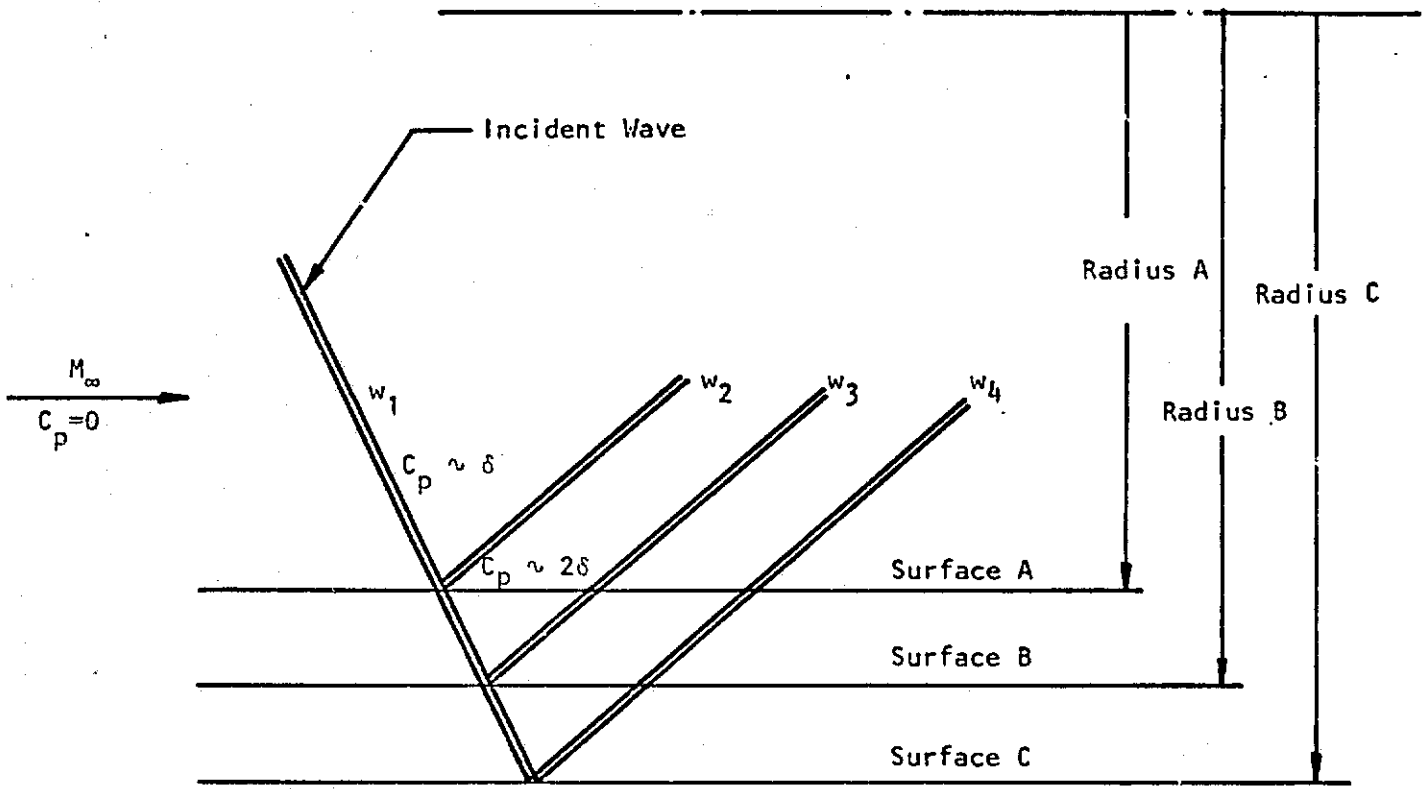

FIGURE 3. WAVE REFLECTION FROM AN IRREGULAR SURFACE

reflection from B is also weakened by the lateral expansion waves which result from the spillover onto C. The last channel, bounded by surface C has no spillover mechanism and so produces the maximum strength reflected wave w_4. However, as soon as w_4 propagates above the channel it is weakened by lateral expansion which strengthens wave w_3. The net result of the process is a diffused set of reflected waves w_2, w_3, w_4, which, in total, produce a pressure perturbation of strength 2δ. However, the fairly slow rate at which waves of the same family intersect one another keeps the individual waves from coalescing for a substantial distance and a gradual expansion of surface C can completely cancel the reflected wave. Thus, the use of a three-dimensional wall geometry such as the corrugated design illustrated in Figure (2) produces a distributed reflection which is well matched to the partial cancellation characteristics of a porous (or slotted) wall and reduces the interfering effect of any uncancelled portion of the wave group which may reach the model. The limiting case of the multigroove wall is, of course, the laterally wavy wall shown in Figure (4) which can be constructed using standard corrugated sheeting. A wall constructed using alternate rows of rods such as that illustrated in Figure (5) is yet another embodiment of the same concept.

In addition to the geometric diffusion produced by the purely inviscid three-dimensional flow effects, the use of a three-dimensional wall geometry can produce geometric diffusion of wall reflections by viscous effects as well. In a real flow system, it is quite difficult to achieve an instantaneous pressure rise by reflecting a wave from a wall. The presence of the wall boundary layer causes the pressure disturbance to propagate upstream, affecting the boundary layer-inviscid flow interaction ahead of the wave reflection point. In the case of a shock or compression wave, the adverse pressure gradient causes a region of local boundary layer separation which extends upstream by a distance which increases as the boundary layer thickness increases. In a supersonic field, this boundary layer separation and subsequent reattachment has the effect of spreading the pressure rise out over an area proportional to the size of the separation region. The use of a three-dimensional wall shape such as that illustrated in Figure (2) produces a considerably increased boundary layer thickness in the corners of the corrugations. This thickened boundary layer produces considerably larger regions of separation than are encountered in a standard design and results in additional streamwise spreading of the waves.

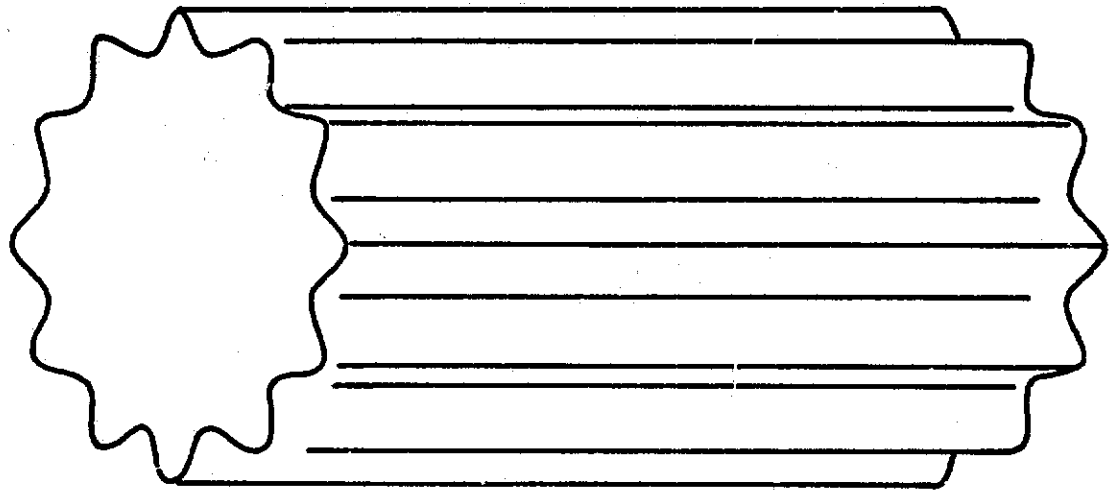

FIGURE 4. WAVY WALL CORRUGATED SECTION

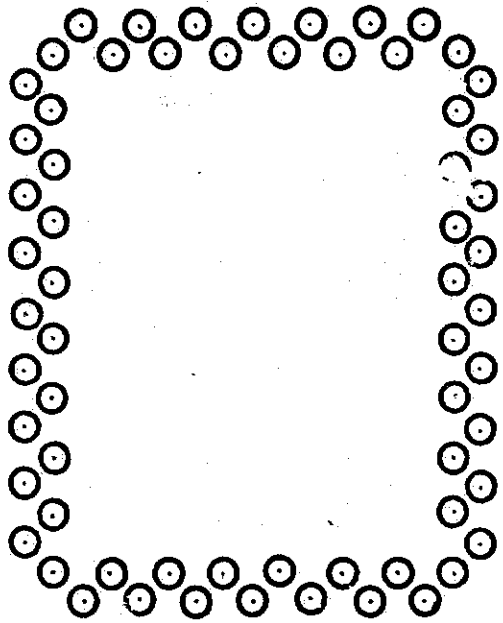

Section A-A

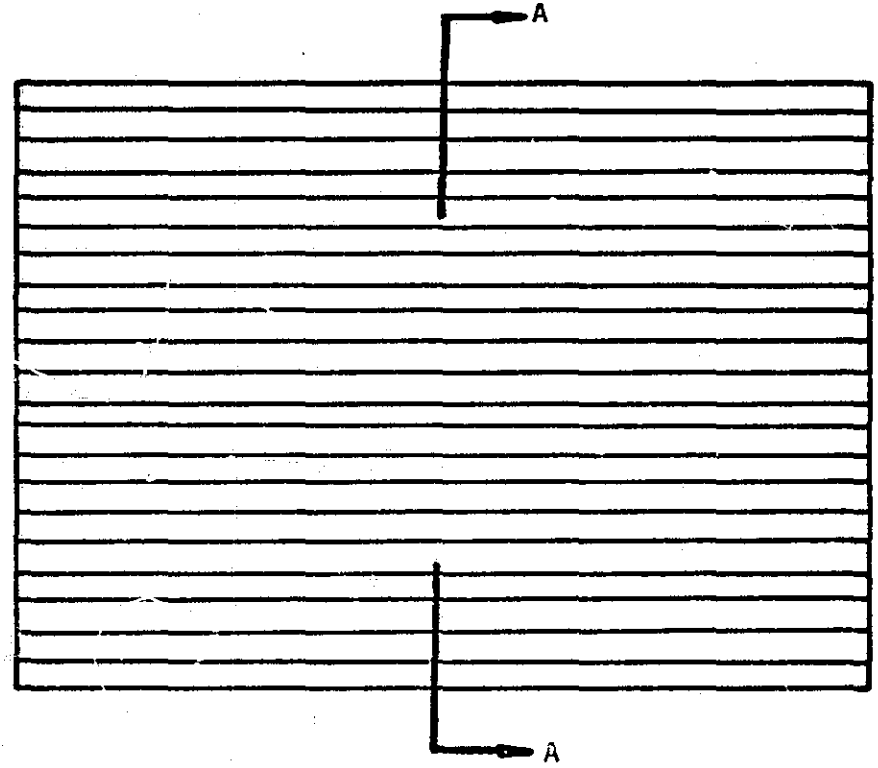

FIGURE 5. DISPLACED ROD WALL SECTION

III. APPARATUS AND PROCEDURES

The transonic test facility utilized in this program is shown in Figure (6). Air enters the settling chamber and passes through a screen pack which removes velocity nonuniformities before entering the convergent nozzle. The constant area test section is provided with a corrugated porous wall surrounded by a low pressure bleed plenum. A cross section of the corrugated test section wall is shown in Figure (7). Air leaving the test section flows through a divergent nozzle which accelerates it to a Mach number of approximately 1.4 before shocking down to a subsonic exit speed. The high velocity test section exhaust air is utilized as an ejector to evacuate a vacuum plenum. Pressure in the bleed plenum is adjusted by regulating the size of the orifices which separate it from the vacuum plenum.

The test section is shown in Figure (8). Its walls are formed by a series of twenty four lands and grooves which run its entire length. The lands and grooves are made of 0.16 mm thickness steel plate with a regular pattern of 0.16 mm diameter holes. The land and groove plates are connected by thin non-porous radial strips.

The test section radius, measured to the surface of the lands, is 67 mm. The grooves are 20 mm deep. A short transition section at the upstream boundary of the test section is formed by a series of alternating ramps leading from the convergent nozzle to the land and groove plates. The ramps are alternately converging and diverging surfaces with respect to the cylindrical entrance nozzle and provide a constant geometric cross sectional area. Two of the land-groove pairs, located 180° apart, are instrumented with static pressure taps to provide wall pressure distributions.

The model used in this program is a 16 mm diameter cylinder with a blunted ogive noise, illustrated in Figure (9), and produces a test section blockage of just over 1%. The model is supported from the rear by a strut mounted in the supersonic section of the exhaust nozzle and is instrumented with static pressure taps starting at the shoulder of the cylindrical section and extending 68 mm downstream. The small diameter of the model made it necessary to install the pressure taps following a helical pattern, so the

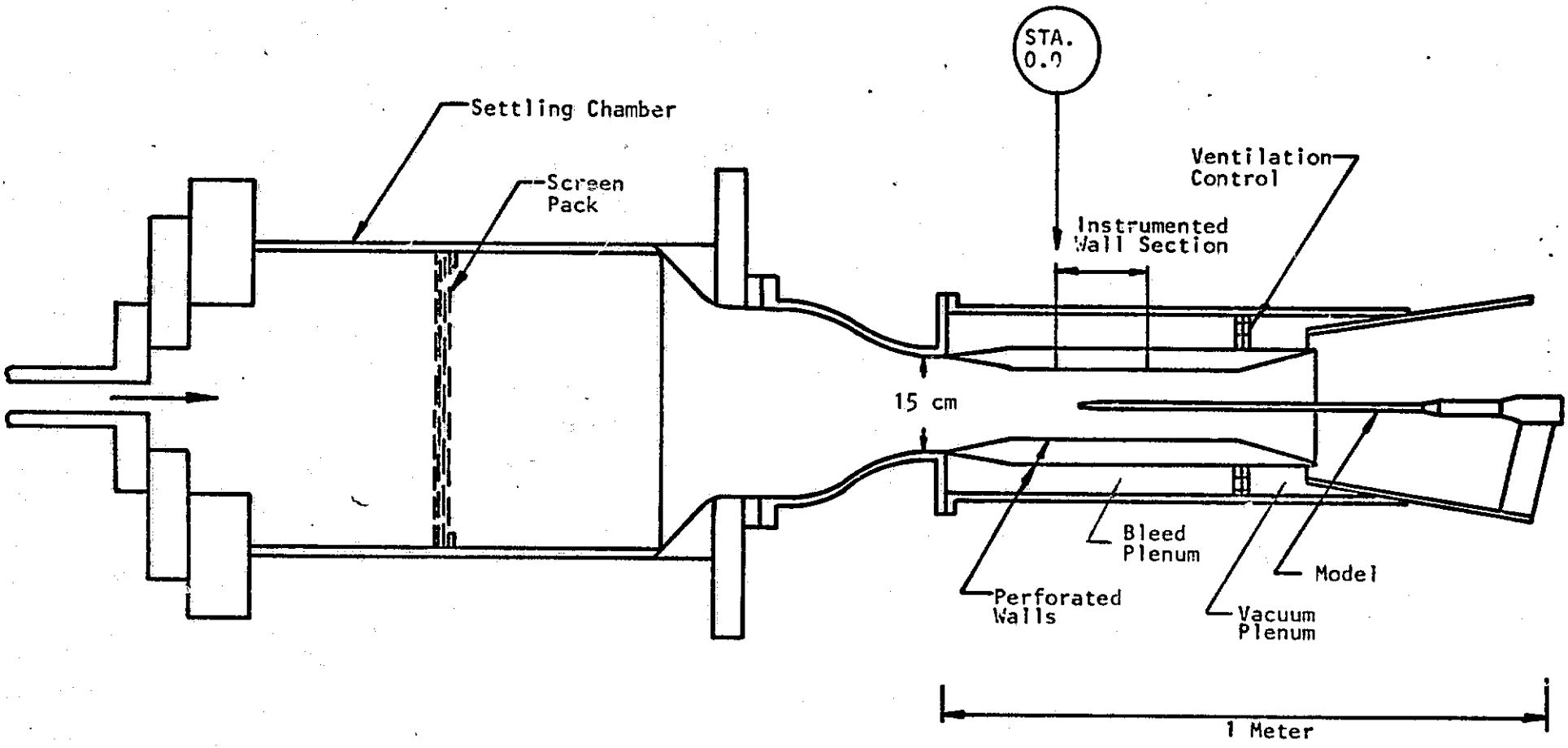

FIGURE 6. TRANSONIC TEST INSTALLATION

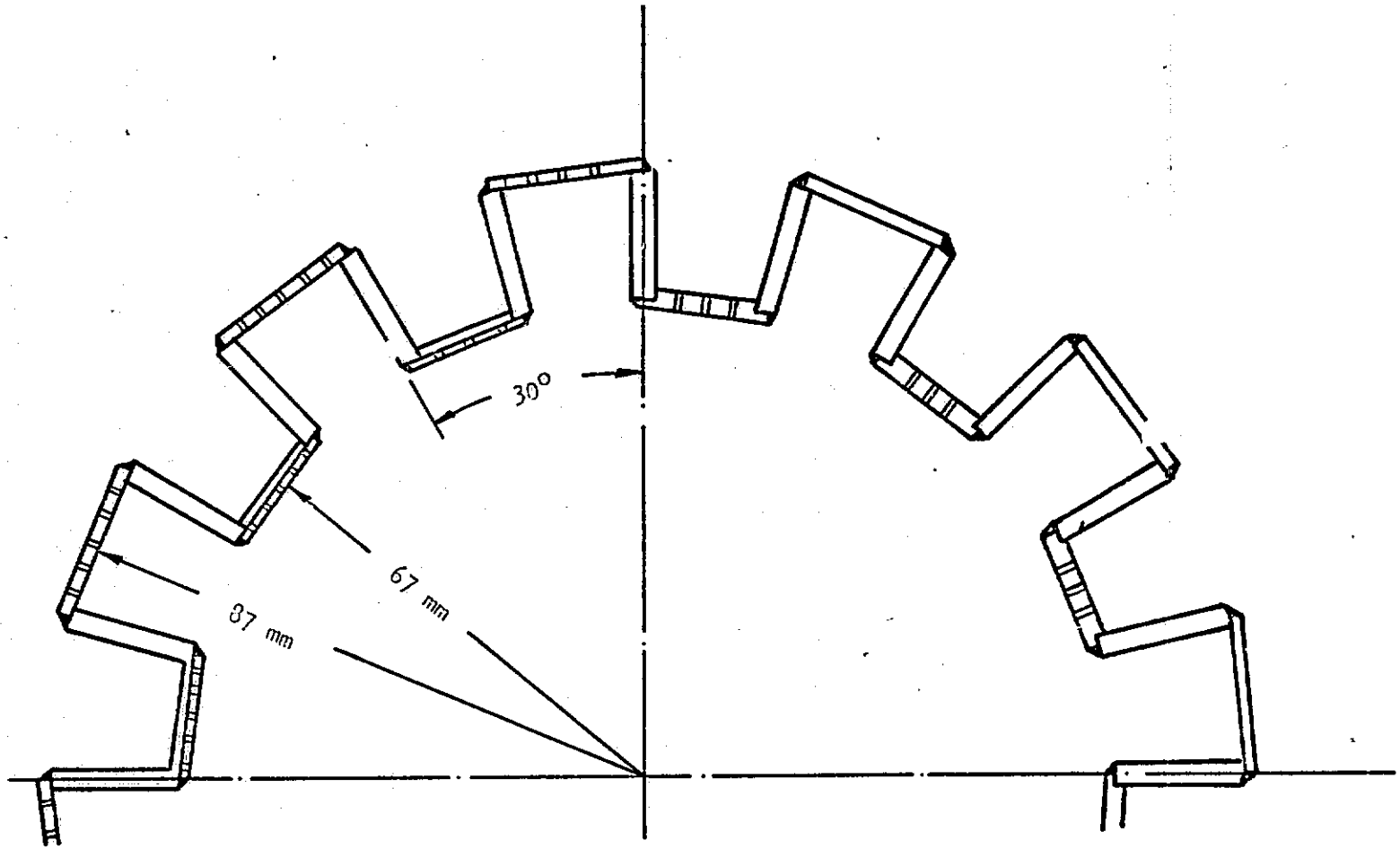

FIGURE 7. CROSS SECTIONAL VIEW OF CORRUGATED WALL TEST SECTION USED IN EXPERIMENTAL PROGRAM

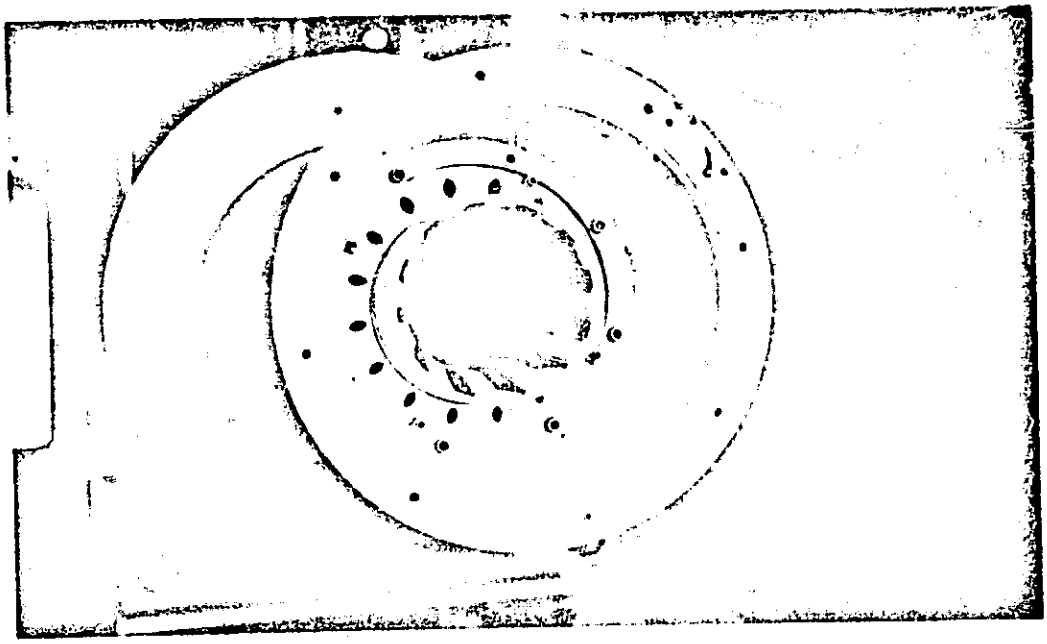

a) Seen from downstream showing ventilation control ring.

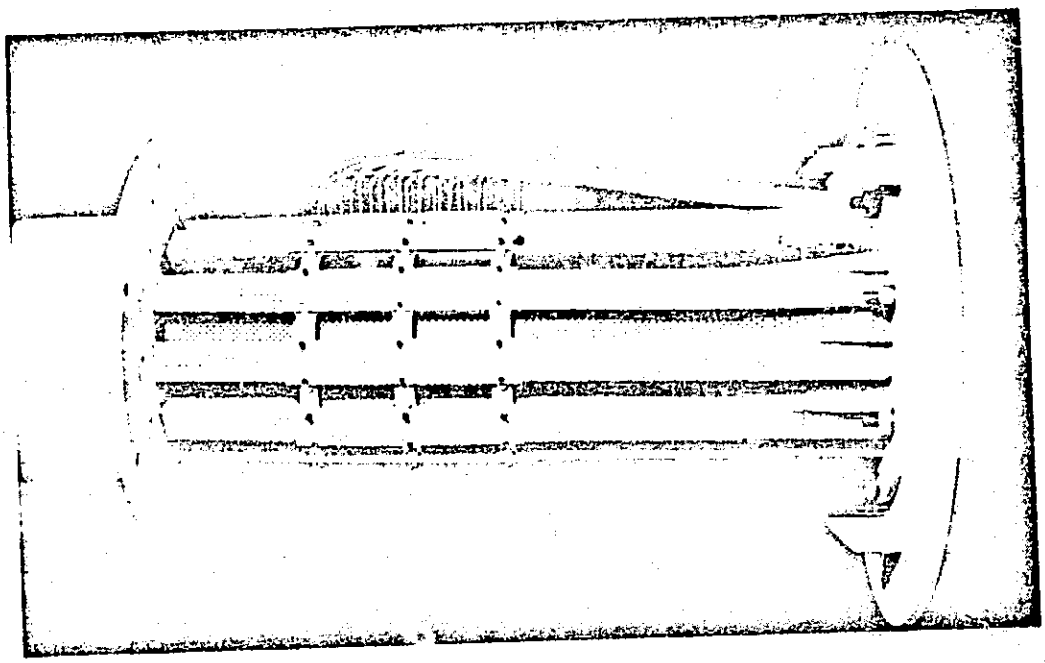

b) As seen from bleed plenum.

FIGURE 8. PERFORATED WALL CORRUGATED TRANSONIC TEST SECTION

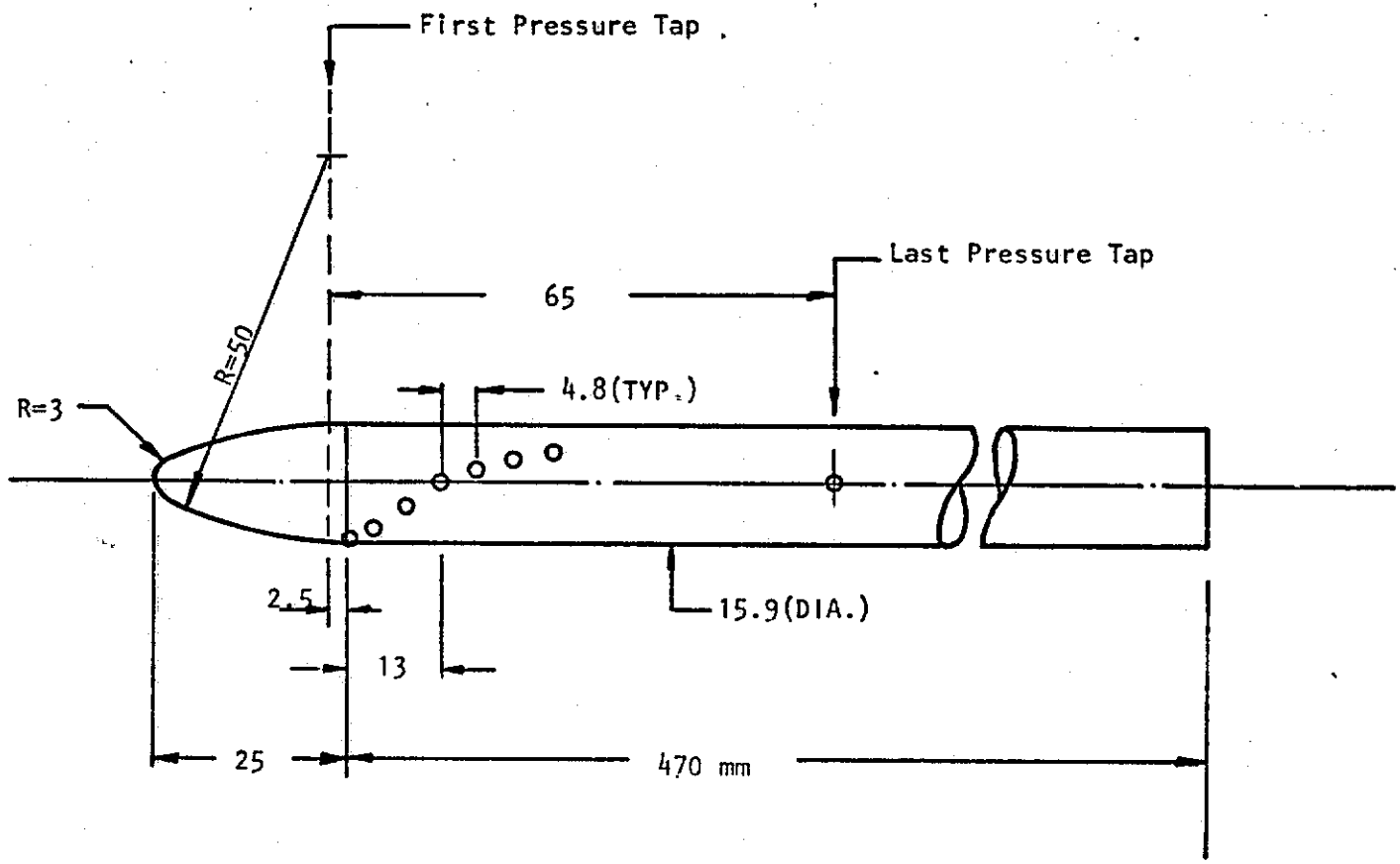

FIGURE 9. MODEL DETAILS (DIMENSIONS IN MILLIMETERS)

taps were spaced at 30^{o} intervals in azimuth, duplicating the repeat pattern of the land-groove arrangement on the corrugated wall.

The initial porosity of the walls was made equal to 16% by utilizing an appropriate pattern of 0.16 mm holes. The porosity was altered during the test program either by decreasing the number of holes in order to decrease porosity in a given region or by enlarging the size of the holes in order to increase the porosity. The basic hole patterns used on the land and groove plates are shown in Figure (10).

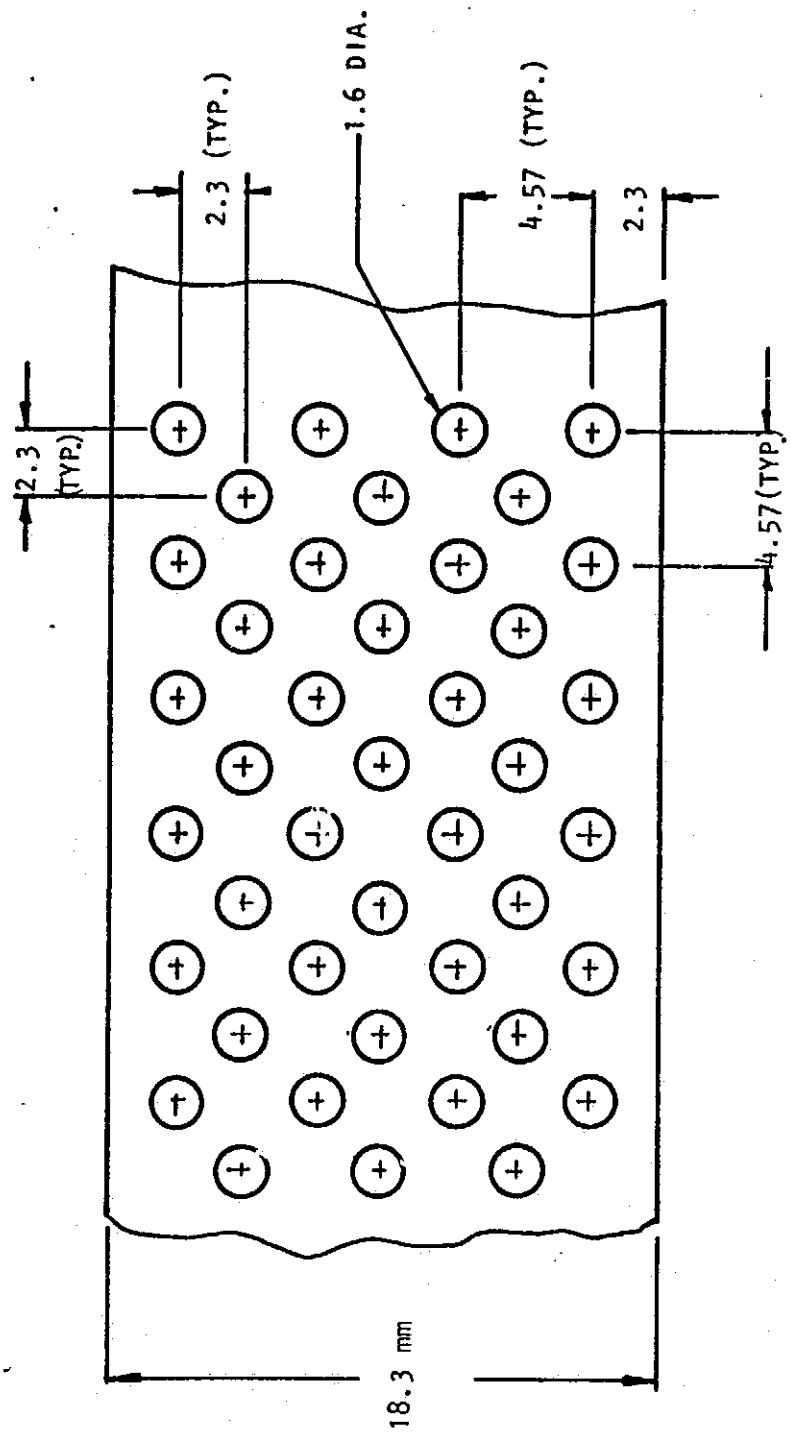

FIGURE 10. BASIC HOLE PATTERN ON POROUS PLATES

IV. EXPERIMENTAL RESULTS

The experimental program had four principal objectives. They were:

1) Demonstrate that a simple three-dimensional wall design will provide the capability to eliminate the bow shock reflection without requiring excessively fine control of the wall porosity distribution.

2) Investigate the effectiveness of porosity control as a means to eliminate wall interference.

3) Investigate the sensitivity of the required wall porosity distribution to free stream Mach number and pressure distribution.

4) Demonstrate that three-dimensional effects produced at the walls diffuse sufficiently rapidly to permit the correction of permeability at a few selected locations along the wall in order to produce a given flow field correction at the center of the test section.

All tests were performed at a constant stagnation pressure of 3 atmospheres using unheated air. The corresponding Reynolds number produced at Mach 1.12 was 4.4×10^{6} m^{-1}. Tunnel calibration was accomplished by replacing the model with an instrumented cylindrical rod of equal diameter extending from the settling chamber through the test section and into the exhaust nozzle. The static pressure distribution along this noseless model and that over the walls was measured and found to be satisfactorily flat. The maximum deviation measured was at the wall and corresponds to $C_p = \pm 0.03$. The free stream Mach number defined by the ratio of bleed plenum to settling chamber pressure was adjusted by movement of the ventilation control plate to change the pressure in the bleed plenum until the desired value was obtained. The range of Mach number investigated was from 1.07 to 1.15 with most testing being carried out at Mach 1.125.

Prior to testing, an analysis was performed to determine the pressure distribution over the model in free flight at Mach number 1.125 as well as the pressure distribution and flow deflection along the lines corresponding to the wall locations. The calculated free flight pressure distributions are shown in Figure (11). The bow shock produced by the model stands approximately one model diameter upstream of the nose and produces a region of subsonic flow which extends approximately halfway along the ogive. The static pressure along the ogive decreases constantly with distance from the stagnation point as the flow accelerates reaching a minimum at the cylindrical shoulder, following which a gradual recompression brings the pressure back to slightly less than the original free stream value. The calculated free flight pressure distributions at radial stations corresponding to the locations of the land and groove surfaces of the corrugated test section wall indicate a sharper and stronger pressure rise occurring along the inner radius with a slight downstream displacement of the pressure distribution at the outer station. Mach lines emanating from the anticipated intersection points of the bow wave with the walls are shown on the figure and indicate that reflection of the bow wave from the land and groove surfaces will perturb the model pressure distribution from the shoulder on downstream.

The calculated flow deflection angles along the land and groove lines are indicated in Figure (12). They show an instantaneous deflection of 1.5^{o} created by the bow wave at the inner wall radius followed by a gradual turn back toward the free stream direction with a small overshoot and subsequent realignment. The shock-induced deflection is displaced slightly downstream at the outer wall radius due to the inclination of the wave and is somewhat weaker than that produced at the inner station. Of interest is the fact that the reflection of shoulder expansion waves from the bow shock creates a condition away from the body where zero C_p no longer implies zero deflection angle, and visa versa. This situation has important implications with regard to the ability of a variable porosity test section to eliminate wall interference and will be discussed later.

Bow Wave Cancellation

Figure (13) shows the measured pressure distribution in the region surrounding the reflection point for a constant porosity wall and a Mach number

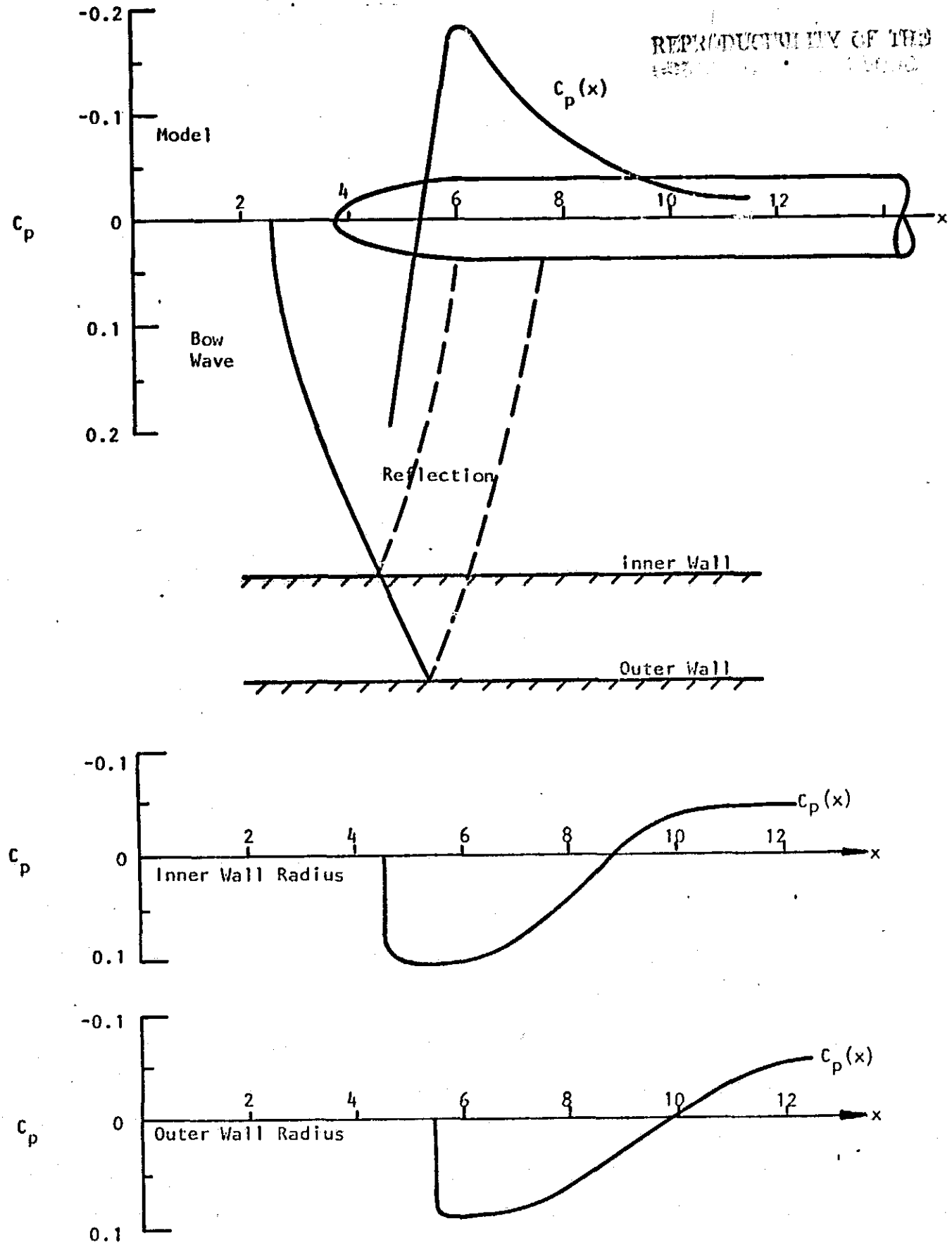

FIGURE 11. CALCULATED FREE FLIGHT FLOW FIELD

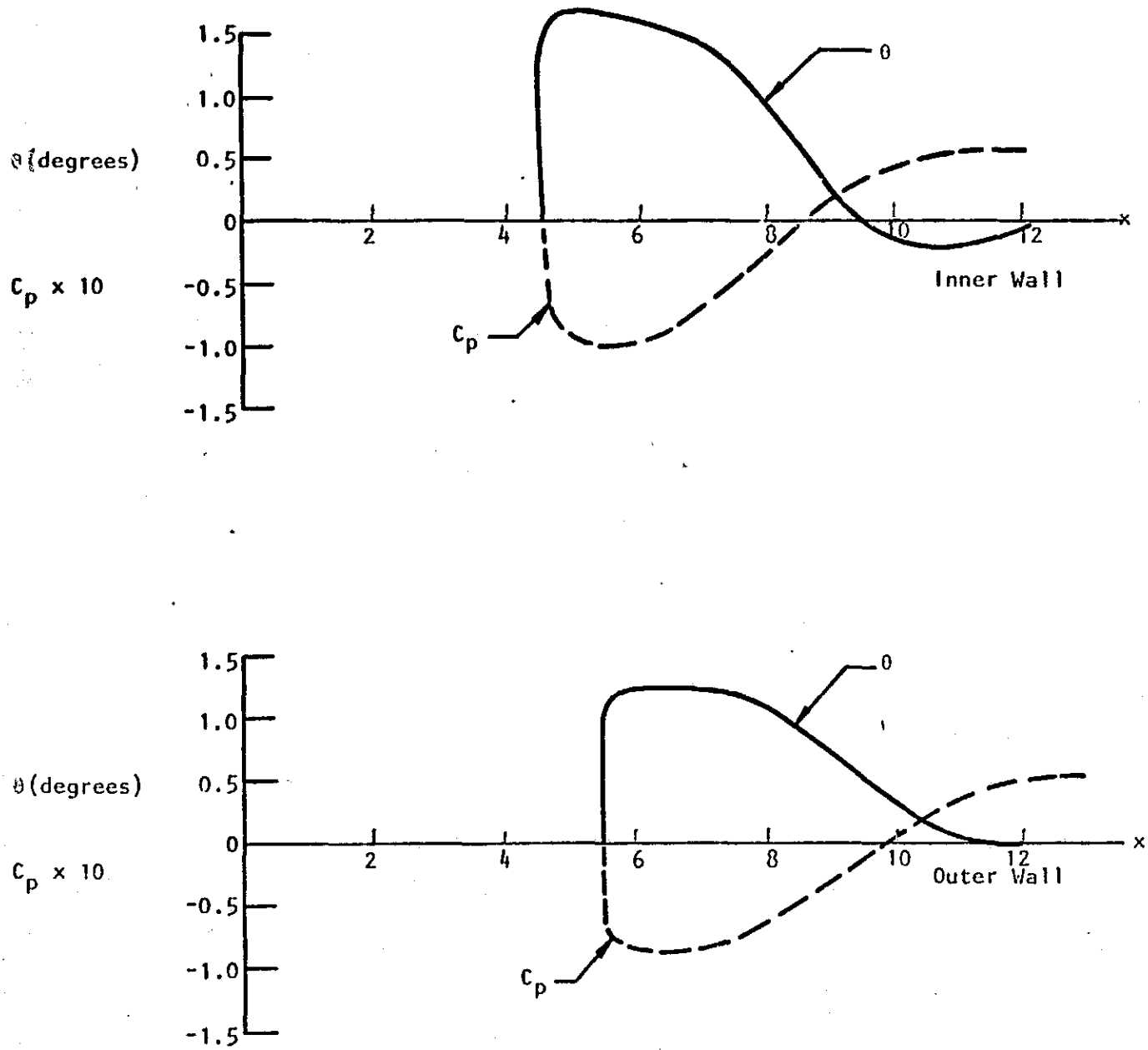

FIGURE 12. CALCULATED FREE FLIGHT PRESSURE AND STREAMLINE INCLINATION AT INNER AND OUTER WALL RADIAL STATIONS

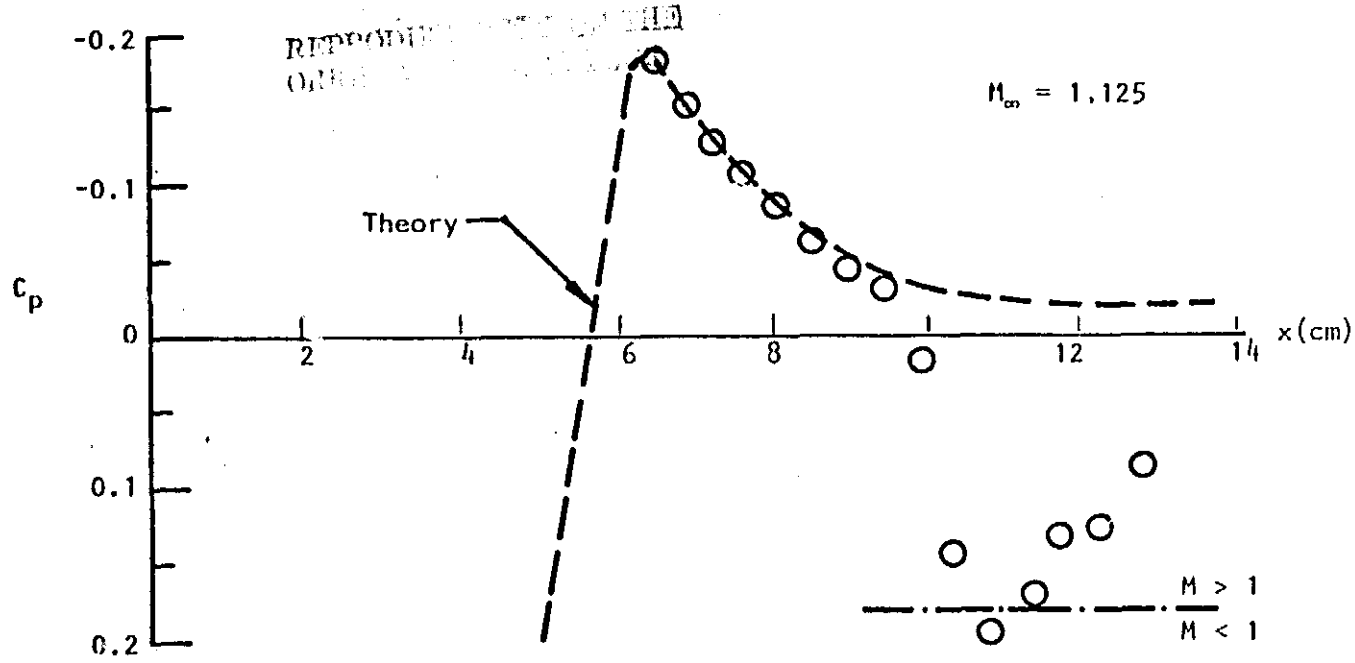

Notes: 1)Wall porosity uniform at 16%

2)% measured from test section entrance station

3)Model nose at x = 3.8

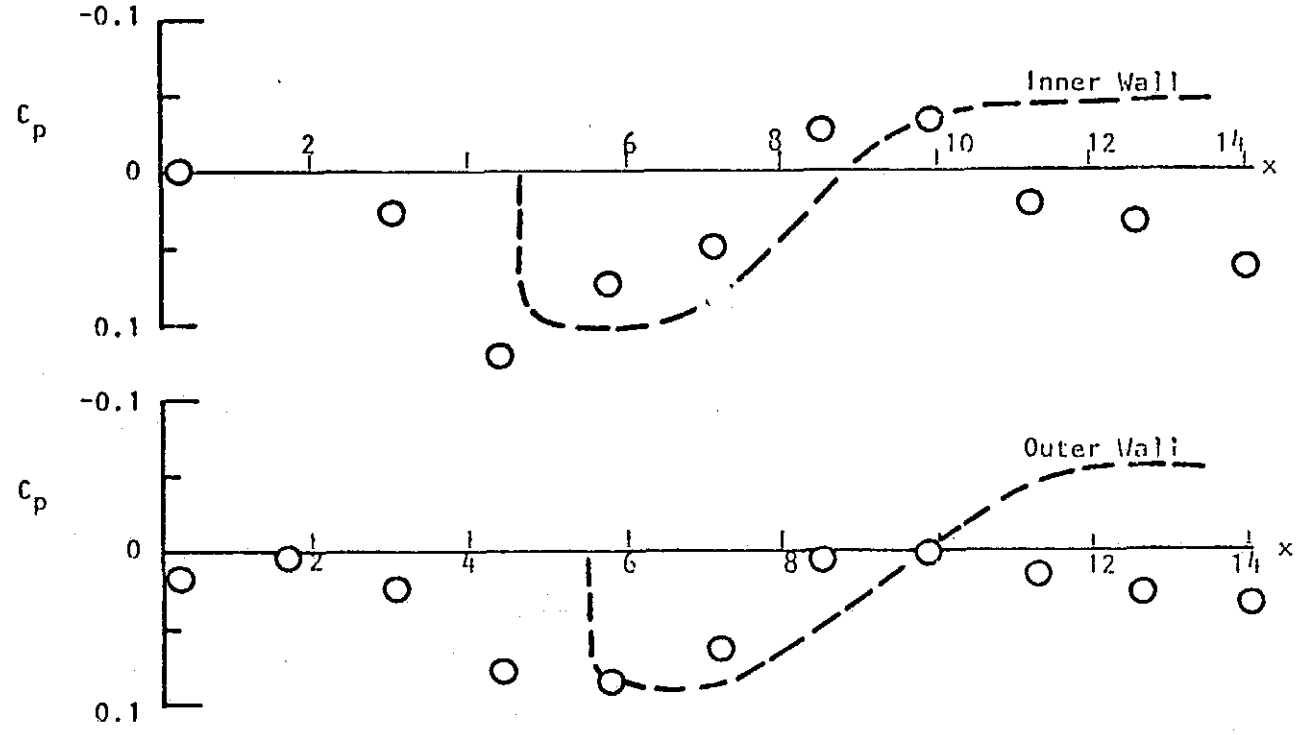

FIGURE 13. MEASURED PRESSURE DISTRIBUTIONS ON MODEL AND INNER AND OUTER TEST SECTION WALLS - UNIFORM POROSITY

of 1.125. The pressure rise measured at the wall is close to the value for zero reflection but is diffused over a distance of approximately 2 cm by the interaction of the boundary layer with the bow shock. Along the wall, the pressure distribution is displaced by approximately one centimeter due to a slightly lower Mach number near the test section boundary. Along the model, there is no sign of a reflected bow wave in the region from station 7 to 10 where one would expect its arrival, indicating that the 16% wall porosity has effectively cancelled the initial reflection. However, an extraneous compression appears at station 10 which, although of only moderate strength along the walls, focuses near the axis to produce locally subsonic flow.

Porosity Control

The ability to affect the pressure distribution over the model by altering the wall porosity distribution is illustrated in Figure (14). In order to reduce the intensity of the focusing disturbance observed on the model at station 10, the land porosity was doubled from station 6 to 7, where C_p was positive, in order to turn the flow further outward. In addition, the land was made impermeable between stations 7 and 10 where the wall pressure coefficient was negative in order to prevent inflow from the plenum. The groove porosity was doubled between stations 5.8 and 7.2 to add to the outflow component. The result of these changes was small along the walls, but quite pronounced on the model. One can see from the figure that the strong recompression at station 10 was completely cancelled by this redistribution of wall permeability. Interestingly, the redistribution of wall porosity still resulted in a strong center compression, this time shifted downstream to station 12. Cancellation of this compression requires further changes in the wall porosity distribution downstream of station 10 on the land and station 8 on the groove surface.

A number of wall porosity distributions were tested, each producing results which confirmed that simple adjustments in wall porosity could be utilized to eliminate unwanted waves near the model. However, there was one very important exception to this finding. It was not possible, regardless of the porosity distribution used, to completely eliminate the unwanted compression in evidence at model station 12. The reason for this lies in the fact that the free flight flow field contains regions where the pressure coefficient

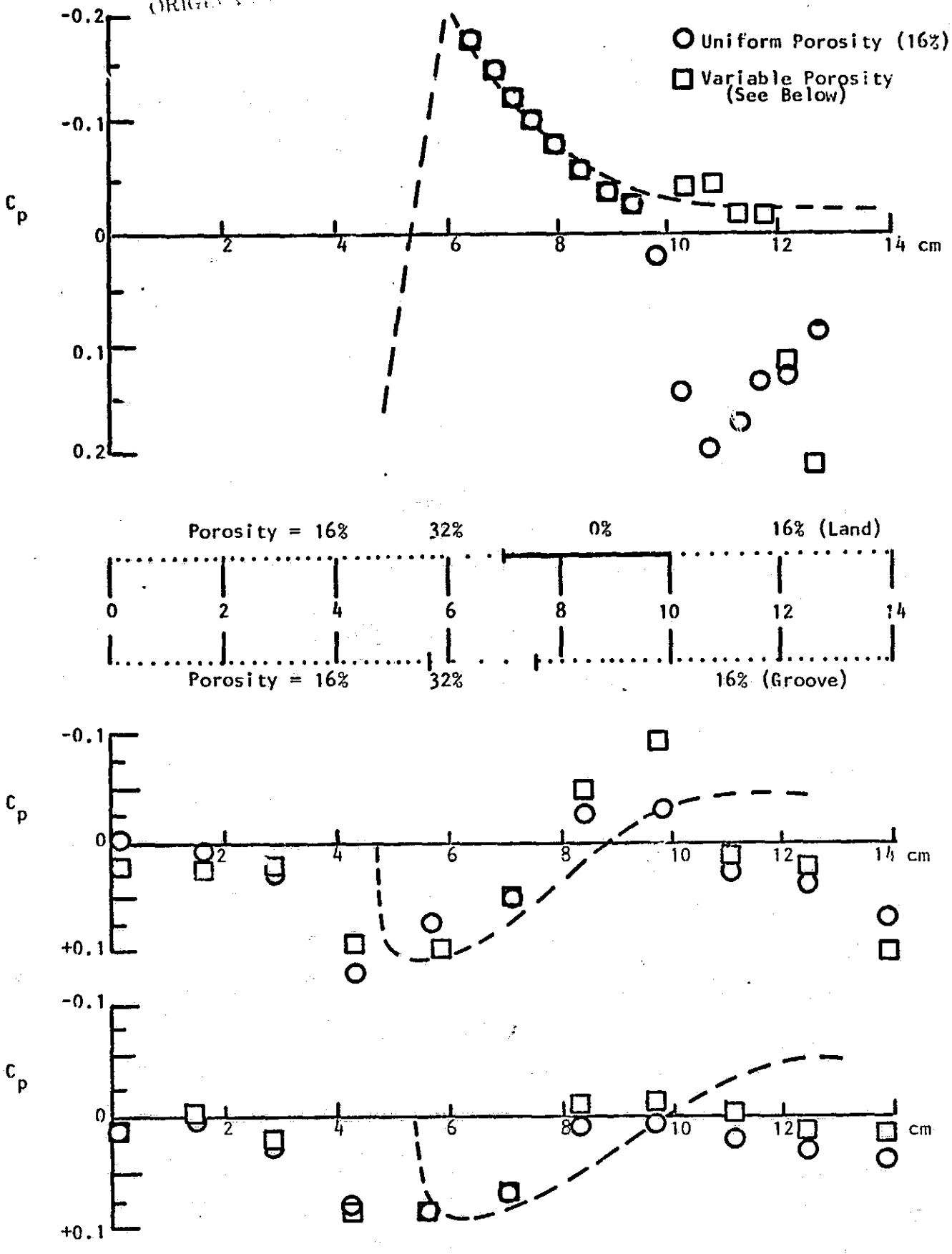

FIGURE 14. CHANGE IN PRESSURE DISTRIBUTION PRODUCED BY VARIABLE POROSITY WALLS (M = 1.125)

is close to zero but a positive flow deflection angle remains. A porous wall requires a finite pressure difference in order to produce cross flow. Since the pressure in a bleed plenum of a constant area test section is, by definition, equal to the free stream pressure, the pressure coefficient along the wall is a direct measure of the wall pressure differential. Therefore, where the wall pressure coefficient approaches zero, the flow must become parallel to the wall. As a result, it is not possible to match the important downstream boundary conditions using a constant area porous test section.

The inability to produce the proper outflow angle as C_p becomes very small results in a series of compression waves originating at the wall and moving out into the test section flow. The intensification of these waves as they approach the center of the axially symmetric flow produces a significant disturbance of the model flow field.

Mach Number Sensitivity

Figures (15) and (16) show the sensitivity of model pressure distribution to free stream Mach number for two different wall porosity distributions. All tests shown were conducted at a Mach number which, to two significant figures, would be reported as 1.1. However, the measurements indicate that the Mach number must be held constant, at least to three significant figures if comparable measurements are to be made. This extreme sensitivity is the result of the large variation in Mach angle which is produced by small changes in Mach number at conditions close to sonic velocity. The changes of Mach angle translate and stretch the pressure distribution which the wall porosity distribution superimposes upon the model flow field.

Diffusion of Three-Dimensional Wall Effects

One of the fundamental questions relating to the use of a non-axially symmetric wall design is its effect on the axial symmetry of the flow around the model. In order to assess the magnitude of this effect, a series of tests were made using a uniform wall porosity of 16%. In these tests, the pressure distribution along the model was first measured with the model in its normal orientation. The model was then rotated through an angle of 5° about its

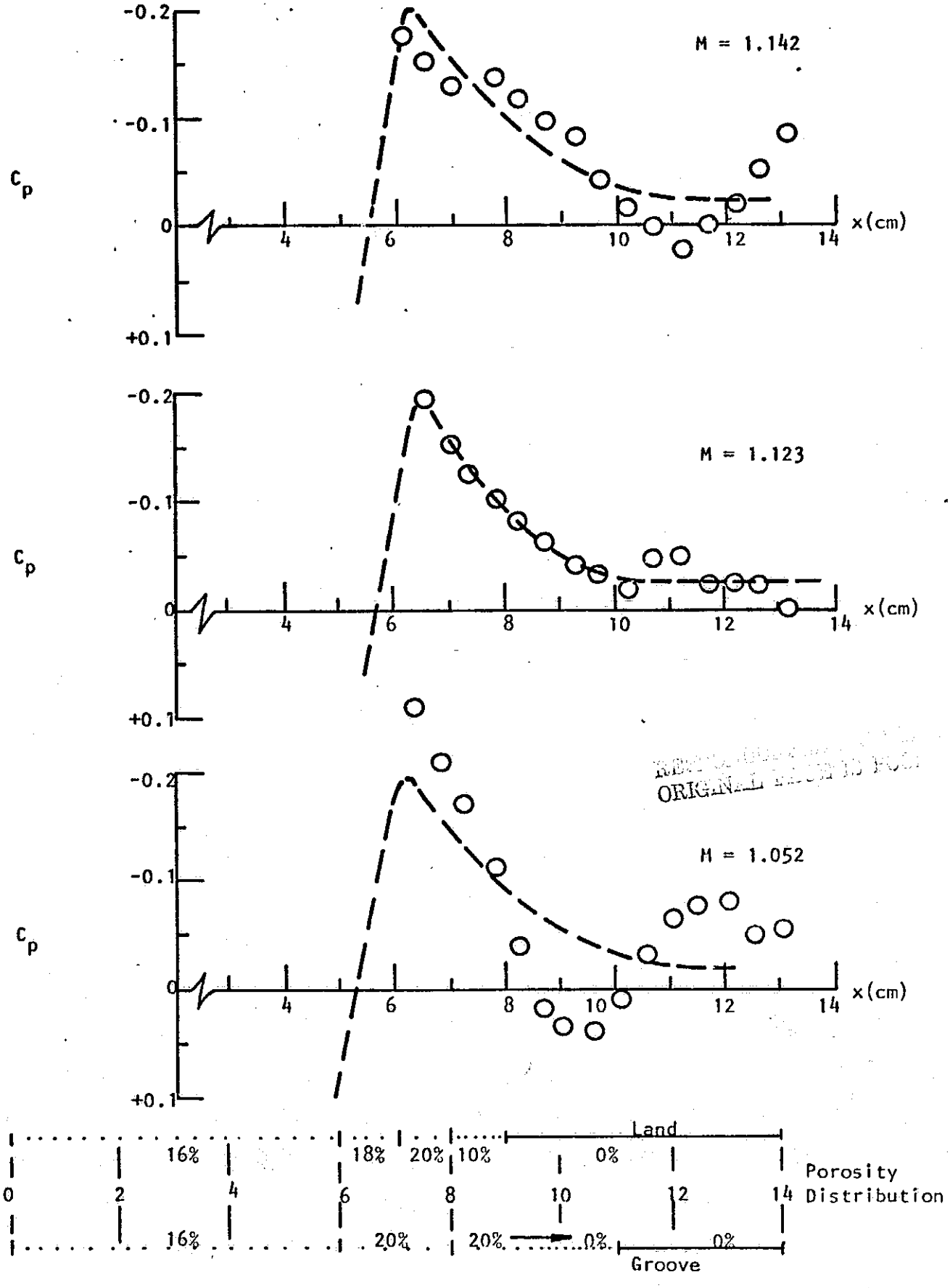

FIGURE 15. EFFECT OF MACH NUMBER PERTURBATION ON MODEL PRESSURE DISTRIBUTION

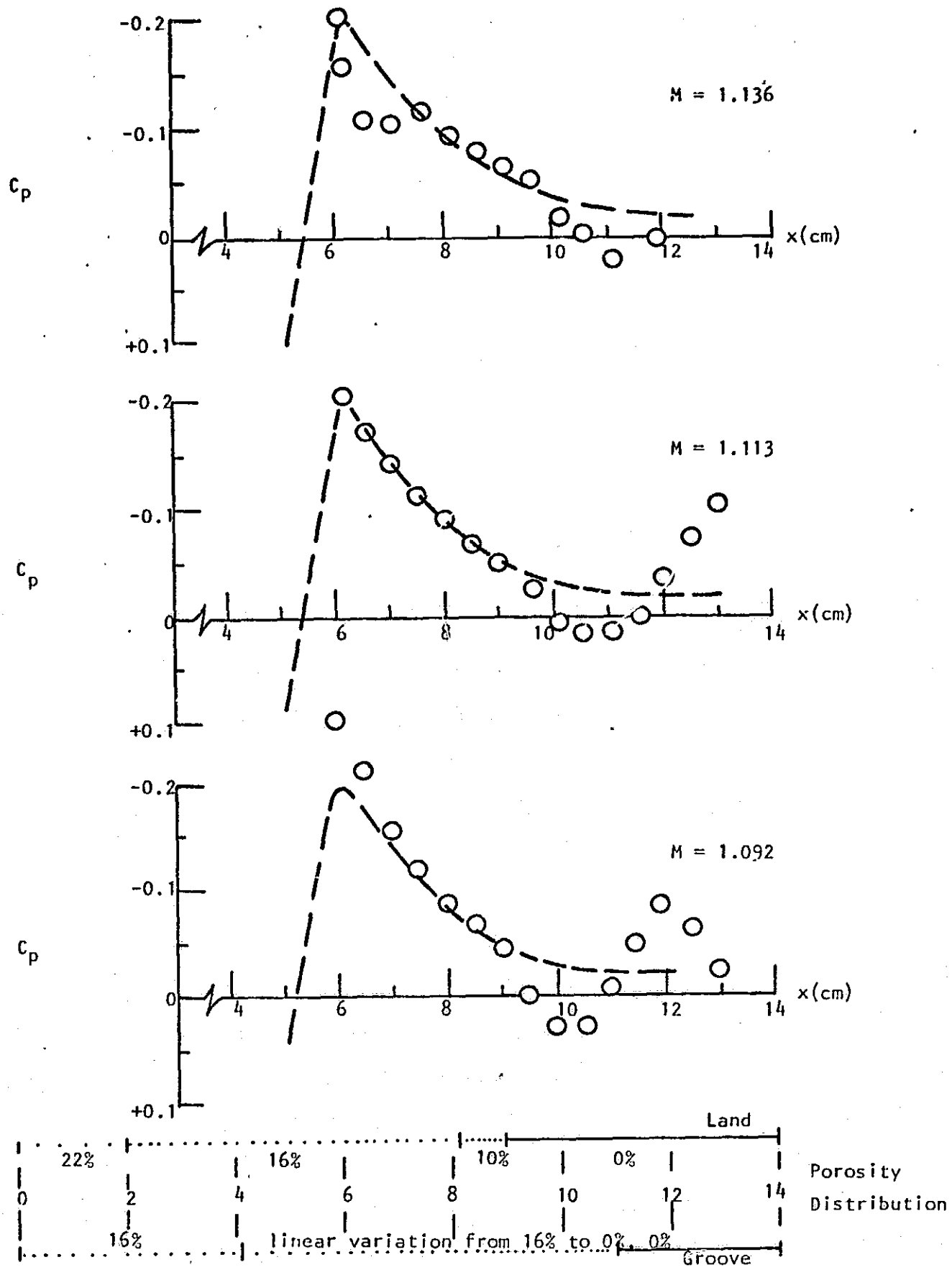

FIGURE 16. EFFECT OF MACH NUMBER PERTURBATION ON MODEL PRESSURE DISTRIBUTION

longitudinal axis and the surface pressure distribution measured again. The measurement was repeated at 5^{o} intervals through the entire 30^{o} arc representing the repeat pattern of the alternating land-groove wall corrugation. The results of these measurements are shown in Figure (17). The figure shows that there is very little variation of pressure coefficient with model orientation indicating good axial symmetry. It should be pointed out that the distance from the wall necessary to achieve axial symmetry is a function of the lateral spacing of the corrugations whereas the degree of wave diffusion which is produced by the corrugations is a function of the groove depth. Since the lateral groove spacing is a function of the test section radius and the angular period of the geometric pattern, the distance to achieve axial symmetry, expressed as a function of the radius, is a function of the angular period alone. For this case, where the angular period is 30^{o}, a model with a radius of 12% that of the inner test section wall can clearly be employed without destroying the axial symmetry of the flow over its surface.

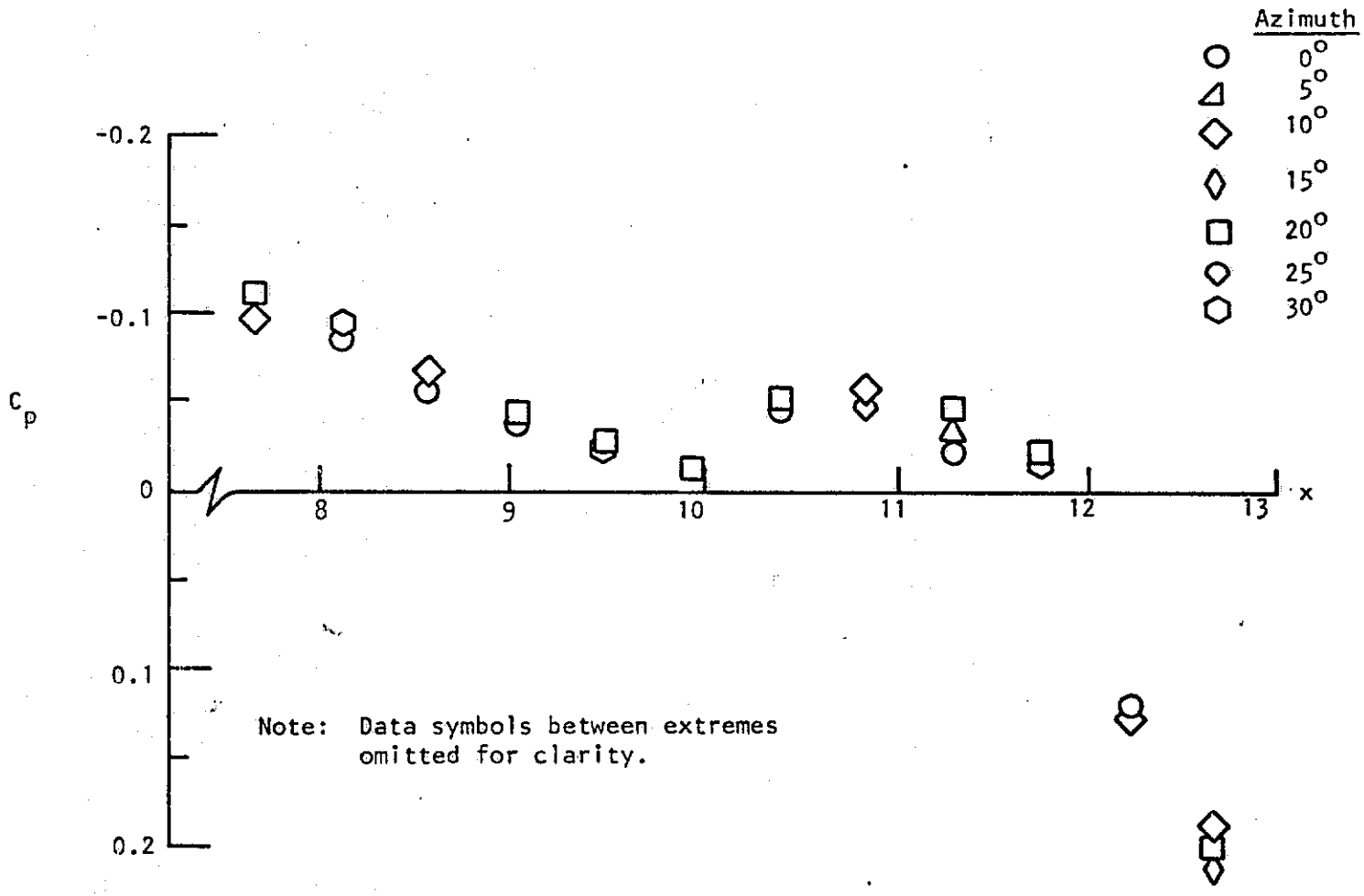

FIGURE 17. MEASURED PRESSURE DISTRIBUTIONS FOR VARIOUS MODEL ROTATIONAL POSITIONS

V. CONCLUSIONS

The results of the experimental program described here point out important directions for low supersonic Mach number wind tunnel test section design which may be summarized as follows:

1) The use of a three-dimensional porous wall can substantially weaken the reflection of the model bow wave system. Although the value of wall porosity required in the initial bow wave reflection zone is a function of the strength of the shock and after-compression, a constant value of porosity across the reflection zone produces good results. Thus, a close tailoring of the wall porosity distribution across the initial reflection zone matching the separate characteristics of the shock and after-compression is not necessary, making the scheme capable of mechanical implementation. The possibility of eliminating shock reflection is an important step for supersonic testing, permitting the use of long bodies in small wind tunnels, provided that the tunnel is designed with variable wall properties.

2) The strongly three-dimensional flow near the wall tends to diffuse rapidly. This result is extremely important as it permits designing wind tunnels where variable geometry is limited to a few wall sections appropriately distributed with respect to the axis of the tunnel. Wall characteristics can be altered in these sections to produce the required corrections in the model region.

3) The well-known focusing effect which causes small disturbances to intensify as they approach the center of an axially symmetric flow tends to amplify small errors in flow direction at the walls to produce major disturbances at the model.

4) A constant area test section cannot accurately reproduce the required boundary conditions along the walls in the region where the pressure coefficient is close to zero. This is due to the outflow characteristics of the porous wall which make it impossible to produce a

finite flow deviation with a corresponding C_p of zero. This difficulty can be overcome by the use of a convergent test section which will increase the pressure differential across the porous walls.